Phase transitions in AgI

Chaok Seok and David W. Oxtoby
Department of Chemistry and James Franck Institute, The University of Chicago, 5640 South Ellis Avenue, Chicago, Illinois 60637
(Received 4 June 1997)

The ordering of silver ions in the superionic conductor α-AgI has been studied using a discrete version of density-functional theory. We obtained a transition to a low-temperature phase different from that found by Madden *et al.* using computer simulations [Phys. Rev. B **45**, 10 206 (1992)]. We suggest that the difference originates from the fact that the I^- lattice is fixed in our study, while the periodic boundary conditions in the simulation allow certain deformations of the I^- lattice on the basis of calculated energies for deformed structures. We therefore argue that the structural change of the I^- lattice and the ordering of Ag^+ ions onto particular sublattices are correlated processes, rather than the ordering of Ag^+ ions driving the $\alpha-\beta$ transition, as suggested by Madden *et al.* The controversial order-disorder transition within the α phase is also discussed in terms of a deformation of the I^- lattice. [S0163-1829(97)01042-4]

I. INTRODUCTION

Silver iodide undergoes a first-order transition from the β phase to the highly conducting α phase at about 420 K at normal pressure. α-AgI is a superionic or fast-ion conductor because it has excess sites for silver ions. In α-AgI, I^- ions form a bcc lattice, and most Ag^+ ions occupy interstitial tetrahedral sites. There are six times as many such sites as Ag^+ ions, and the ions can move among the sites by crossing a low-energy barrier. In β-AgI, I^- ions have the hcp structure, and Ag^+ ions are tetrahedrally coordinated to I^- (wurtzite structure). In addition to the $\alpha-\beta$ transition, an order-disorder transition has been proposed to occur within the α phase by Perrott and Fletcher.[1] They observed a heat-capacity change at about 700 K like those in first-order phase transitions. Raman-scattering intensity and depolarization ratio measurements around that temperature[2] and changes in elastic constants determined by Brillouin scattering[3] also support the suggestion. There are some contradictory experiments, however.[4]

The phase diagram of AgI over a wide range of temperature and pressure, including the $\alpha-\beta$ transition, has been investigated using a constant stress molecular-dynamics simulation.[5,6] Tallon[6] found a heat-capacity change in the simulation like that observed experimentally.

Szabó[7] studied the phase transition in α-AgI using a mean-field theory for a lattice gas with nearest- (NN) and next-nearest-neighbor (NNN) interactions. He considered only tetrahedral interstitial sites which are known to have the highest occupancies, and redivided them into six interpenetrating bcc sublattices, as in Fig. 1. A disordered state is stable at high temperature, and an ordered state where only one sublattice is occupied (D phase) was found to be stable at low temperature. Partially ordered intermediate phases were also found, and he argued that these phases might explain the heat-capacity and Raman experiments.

More recently, Madden and co-workers[8] showed that in a molecular-dynamics (MD) simulation with a simulation box of fixed shape and size, Ag^+ ions undergo a second-order order-disorder transition at about 400 K, although the I^- lattice structure cannot change from bcc. There was no evidence for an order-disorder transition within the α phase. Figure 2 shows the structure of the low-temperature ordered phase (M phase). These authors noted the structural similarity of the M phase and β-AgI, and showed that gliding of alternate (110) planes of I^- in the M phase with contraction of the cell can lead to the wurtzite structure of the β phase (see Fig. 3), as in the Burgers mechanism for a transition from bcc to hcp.[9] Because the ordered M phase occurs when the change of bcc to hcp of the I^- lattice is prevented, they argued that the ordering tendency of Ag^+ ions in the α phase is the driving force for the $\alpha-\beta$ phase transition.

We have studied this ordering transition of Ag^+ in α-AgI using a lattice version of the density-functional approach. In our model, I^- ions are fixed in a perfect bcc lattice, and Ag^+ ions are restricted to tetrahedral interstitial sites, as in Szabó's study. However, the more realistic potential model used in simulations is employed (see Sec. III). The direct correlation functions are calculated from the hypernetted

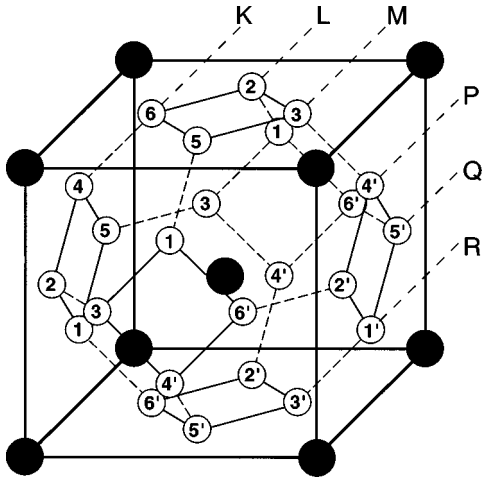

FIG. 1. Six sublattices of tetrahedral sites (with $i=i'$) introduced by Szabó. Black circles represent I^- ions and white circles T_d sites. The 12 sublattices (with $i\neq i'$) will be discussed later in the text. K, L, ..., and R denote planes parallel to (110), and repeat in space. K planes consist of sublattices 4 and 6, and P of $4'$ and $6'$, etc.

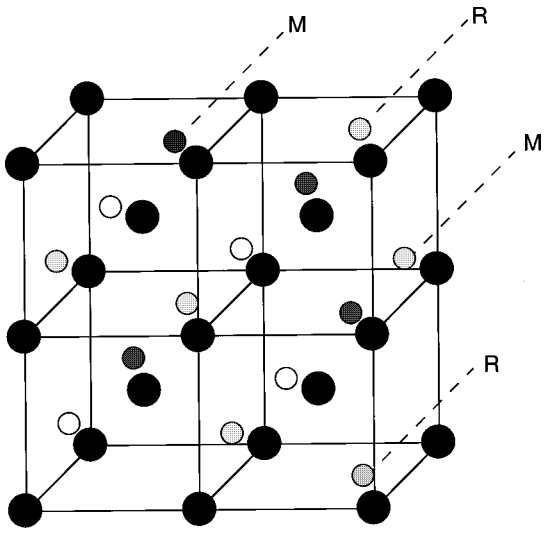

FIG. 2. Structure of the M phase. Szabó type-1 sites in M planes (sublattice 1) and type-3 sites in R planes (sublattice $3'$) are occupied in this ordered state. Black circles represent I^- ions and white ones Ag^+ ions.

chain (HNC) closure or Monte Carlo (MC) simulation. Our results turned out to be different from what was expected from the MD simulation of Ref. 8, however. Ag^+ ions become ordered in the D phase instead of M at low temperature. Among the many approximations made in our calculations, the most important one, different from those in Ref. 8, is that ions are restricted to particular lattice sites. We argue that a small hcp-like deformation of the I^- lattice from bcc that is compatible with the cubic periodic boundary condition (a deformation allowed in Madden's simulation but not allowed in our study) may be responsible for the transition to the M phase. Therefore, the $\alpha-\beta$ transition may not be driven by the ordering transition of Ag^+ alone, but by a correlated structural change of I^- and ordering of Ag^+ that occur simultaneously. The possibility of an order-disorder transition within the α phase is discussed in terms of a structural deformation.

The outline of this paper is as follows. In Sec. II, the density-functional theory applied to the α-AgI system is described, and the results obtained by the HNC closure and MC simulation are presented in Secs. III and IV. In Sec. V, the difference between our results and those of Ref. 8 is discussed, and the possible role of a deformation of the I^- lattice is suggested. A future extension of this study to incorporate the structural change of the I^- lattice is proposed in Sec. VI.

II. DENSITY-FUNCTIONAL APPROACH

We consider the phase transition of Ag^+ ions restricted to the tetrahedral (T_d) sites when I^- ions are fixed in a perfect bcc lattice. We divide the T_d sites into 12 sublattices, as in Fig. 1, to incorporate the symmetry of the M phase (where 1 and $3'$ are occupied) as well as D (where 1 and $1'$ are occupied). Let the occupation number for each of the 12 sublattices be n_i ($i=1,2,\ldots,12$). The Helmholtz free energy is expanded around the disordered state where $n_i \equiv n_0 = 1/6$, and truncated at the pair direct correlation function level, as

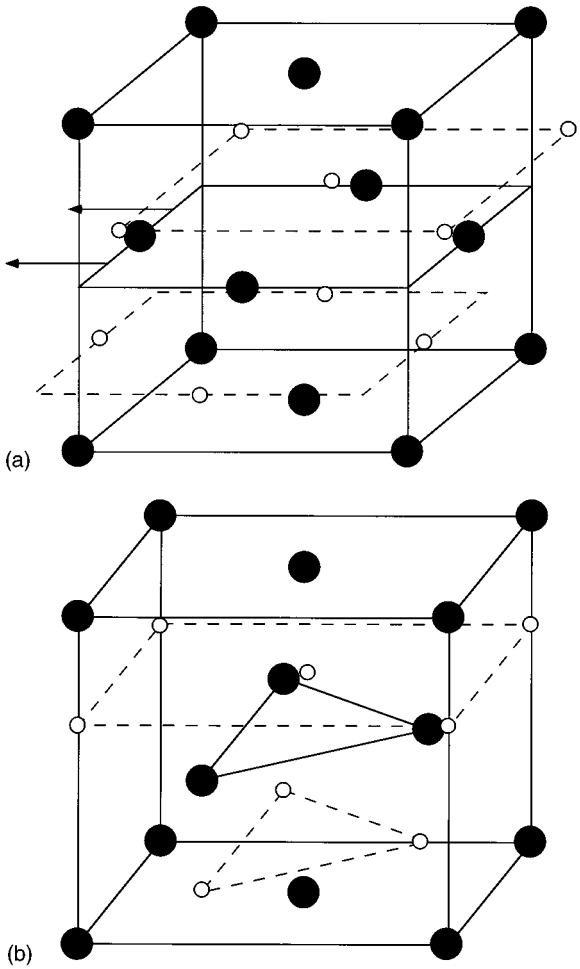

FIG. 3. (a) (110) planes of the M phase. Gliding of alternate layers is indicated by arrows on the left. In going from the M phase to the β phase, tetrahedral coordination of Ag^+ to I^- should be maintained. (b) Corresponding planes of the β phase. I^- ions now form an hcp lattice.

in the lattice analog of density-functional theory described in Ref. 10. The Helmholtz free-energy difference between the ordered and disordered phases is

$$\frac{\beta}{N}\Delta F = \sum_{i=1}^{12} [S(n_i) - S(n_0)] - \frac{1}{2}\sum_{i=1}^{12}\sum_{j=1}^{12} \overline{c_{ij}}(n_i - n_0)(n_j - n_0), \tag{1}$$

where

$$S(n) = n \ln n + (1-n)\ln(1-n), \tag{2}$$

and

$$\overline{c_{ij}} = \sum_{L=1}^{N} c_{i1,jL}. \tag{3}$$

$c_{i1,jL}$ is the direct correlation function of Ag^+ for the separation of site i in the 1st cell and site j in the Lth cell. N is the number of unit cells of the bcc I^- lattice, which is half

TABLE I. Equivalent $\overline{c_{ij}}$'s.

$\overline{c_{ij}}$	Equivalent $\{ij\}$					
$\overline{c_{11}}$	11	22	33	44	55	66
$\overline{c_{12}}$	12,15	21,23,24,26	32,35	42,45	51,53,54,56	62,65
$\overline{c_{13}}$	13		31	46		64
$\overline{c_{14}}$	14,14′		36,36′	41,41′		63,63′
$\overline{c_{16}}$	16		34	43		61
$\overline{c_{11'}}$	11′	22′	33′	44′	55′	66′
$\overline{c_{12'}}$	12′,15′	21′,23′,24′,26′	32′,35′	42′,45′	51′,53′,54′,56′	62′,65′
$\overline{c_{13'}}$	13′		31′	46′		64′
$\overline{c_{16'}}$	16′		34′	43′		61′
$\overline{c_{25}}$		25			52	
$\overline{c_{25'}}$		25′			52′	

the number of silver ions. The first derivative of the excess free-energy term is zero because $\Sigma_i(n_i-n_0)=0$.

Equilibrium occupation numbers are obtained by minimizing ΔF, giving

$$n_i=\frac{1}{1+\exp\left[-\gamma-\sum_j \overline{c_{ij}}(n_j-n_0)\right]}, \tag{4}$$

where the undetermined multiplier γ is fixed by the condition $\Sigma_{i=1}^{12}n_i=2$. Because of the symmetry of the lattice, some $\overline{c_{ij}}$ are equivalent to each other, as shown in Table I. Note that $\overline{c_{ij}}=\overline{c_{ji}}=\overline{c_{i'j'}}=\overline{c_{j'i'}}$ and $\overline{c_{ij'}}=\overline{c_{i'j}}$. In addition to $\overline{c_{ij}}$, we also define $\widetilde{c}_{ij}$, the sum of the direct correlation functions between Szabó's sublattice i and j, as follows:

$$\widetilde{c}_{ij}=\overline{c_{ij}}+\overline{c_{ij'}}=\frac{1}{2}(\overline{c_{ij}}+\overline{c_{ij'}}+\overline{c_{i'j}}+\overline{c_{i'j'}}). \tag{5}$$

There are only three different $\widetilde{c}_{ij}$'s ($\widetilde{c}_{11}=\widetilde{c}_{22}=\ldots$, $\widetilde{c}_{14}=\widetilde{c}_{25}=\widetilde{c}_{36}$, and $\widetilde{c}_{12}=\widetilde{c}_{13}=\ldots$). Any i and i' form a bcc lattice together, and $\widetilde{c}_{ii'}=\widetilde{c}_{11}$. If i and j sublattices have nearest neighbors on each other, $\widetilde{c}_{ij}=\widetilde{c}_{12}$, and if they have next-nearest neighbors, $\widetilde{c}_{ij}=\widetilde{c}_{14}$.

Let us consider the states studied by Szabó[7] first. These states have a symmetry such that $n_i=n_{i'}$, and the following occupation numbers :

$$\begin{aligned} n_1&=n_{1'}=n_0+v+w+x+y+z,\\ n_2&=n_{2'}=n_0-v,\\ n_3&=n_{3'}=n_0-w,\\ n_4&=n_{4'}=n_0-x,\\ n_5&=n_{5'}=n_0-y,\\ n_6&=n_{6'}=n_0-z. \end{aligned} \tag{6}$$

Because of the symmetries of $\overline{c_{ij}}$ and $\widetilde{c}_{ij}$, there are only two linear combinations of $\overline{c_{ij}}$'s that matter in the Szabó states:

$$a_1=\widetilde{c}_{11}+\widetilde{c}_{14}-2\widetilde{c}_{12}, \tag{7}$$

$$a_2=\widetilde{c}_{11}-\widetilde{c}_{14}. \tag{8}$$

The terms $\Sigma_j\overline{c_{ij}}(n_j-n_0)$ which appear in Eq. (4) can be written as follows:

$$\begin{aligned} 2\sum_j \overline{c_{1(1')j}}(n_j-n_0)&=(a_1+a_2)(v+w+x+y+z)+2a_2x,\\ 2\sum_j \overline{c_{2(2')j}}(n_j-n_0)&=-(a_1+a_2)v-(a_1-a_2)y,\\ 2\sum_j \overline{c_{3(3')j}}(n_j-n_0)&=-(a_1+a_2)w-(a_1-a_2)z,\\ 2\sum_j \overline{c_{4(4')j}}(n_j-n_0)&=(a_1-a_2)(v+w+x+y+z)-2a_2x,\\ 2\sum_j \overline{c_{5(5')j}}(n_j-n_0)&=-(a_1-a_2)v-(a_1+a_2)y,\\ 2\sum_j \overline{c_{6(6')j}}(n_j-n_0)&=-(a_1-a_2)w-(a_1+a_2)z. \end{aligned} \tag{9}$$

n_i and ΔF can be calculated from the above and Eqs. (4) and (1). The above equations look similar to those in Ref. 7, and a_1 and a_2 can be expressed in terms of the nearest- and next-nearest potential parameters used in that reference. However, the effective NN and NNN interaction potentials summed over all lattice sites diverge in the case of a Coulomb potential, whereas a_1 and a_2 are well behaved because the infinite parts are subtracted out by the linear combinations that define them.

We now consider an ordered phase with the symmetry of the M phase. If $n_1=n_{3'}$, it follows that

$$\begin{aligned} n_1&=n_{3'}=n_0+2w+x+y+z,\\ n_2&=n_{2'}=n_5=n_{5'}=n_0-w,\\ n_3&=n_{1'}=n_0-x,\\ n_4&=n_{6'}=n_0-y,\\ n_6&=n_{4'}=n_0-z. \end{aligned} \tag{10}$$

There are two additional linear combinations of $\overline{c_{ij}}$'s that appear in the final equations in this case:

$$a_3=\overline{c_{11}}-\overline{c_{11'}}-\overline{c_{13}}+\overline{c_{13'}}, \tag{11}$$

$$a_4=\overline{c_{16}}-\overline{c_{16'}}. \tag{12}$$

We now find

$$\begin{aligned}
2\sum_j \overline{c_{1(3')j}}(n_j-n_0)&=-(a_1+a_2+2a_3)w-2a_3x\\
&\quad-(a_2+a_3+a_4)y-(a_2+a_3-a_4)z,\\
2\sum_j \overline{c_{2(2',5,5')j}}(n_j-n_0)&=2a_1w,\\
2\sum_j \overline{c_{3(1')j}}(n_j-n_0)&=-(a_1+a_2-2a_3)w+2a_3x\\
&\quad-(a_2-a_3-a_4)y-(a_2-a_3+a_4)z,\\
2\sum_j \overline{c_{4(6')j}}(n_j-n_0)&=-(a_1-a_2-2a_4)w+2a_4x\\
&\quad+(a_2+a_3+a_4)y+(a_2-a_3+a_4)z,\\
2\sum_j \overline{c_{6(4')j}}(n_j-n_0)&=-(a_1-a_2+2a_4)w-2a_4x\\
&\quad+(a_2-a_3-a_4)y+(a_2+a_3-a_4)z.
\end{aligned} \tag{13}$$

III. THE HNC CLOSURE

We employ the following pair potential model used in the computer simulations:[5,6,8]

$$\begin{aligned}
V_{\mathrm{AgAg}}(r)&=\frac{0.014804}{r^{11}}+\frac{0.36}{r},\\
V_{\mathrm{AgI}}(r)&=\frac{114.48}{r^9}-\frac{0.36}{r}-\frac{1.1736}{r^4},\\
V_{\mathrm{II}}(r)&=\frac{446.64}{r^7}+\frac{0.36}{r}-\frac{2.3472}{r^4}-\frac{6.9331}{r^6},
\end{aligned} \tag{14}$$

where lengths are in Å and energies in $e^2/$ Å$=14.40$ eV. The above potential has been very successful in reproducing the α–β transition. Because the I^- lattice is fixed and all Ag^+ sites are equivalent, only V_{AgAg} is used here. We ignore the $1/r^{11}$ term which is smaller than the $1/r$ term by a factor of 10^{-4} at the separation between the nearest tetrahedral sites. The lattice parameter $a=5.206$ Å is used, as in Ref. 8.

The simplest way to calculate the direct correlation functions a_1–a_4 is through a simple mean-field approximation. Although we shall see that this gives unsatisfactory results, it is worth presenting first. In this approximation,

$$\begin{aligned}
c_{i1,jL}&=0 \ \text{ if } \ i=j \ \text{ and } L=1\\
&\quad-\beta v_{i1,jL} \ \text{ otherwise,}
\end{aligned} \tag{15}$$

where $v_{i1,jL}=V_{\mathrm{AgAg}}(r_{i1,jL})$. Szabó's calculation consists of such a mean-field approximation, together with a further restriction to near-neighbor interactions. For the full long-range potential, each $\overline{c_{ij}}$ alone does not converge if the $c_{i1,jL}$ are summed over the infinite lattice, but a_1–a_4 can be obtained as follows. For example, a_1 can be written by using relationships of the $\tilde{c}_{ij}$'s:

$$\begin{aligned}
a_1=\tilde{c}_{11}+\tilde{c}_{14}-2\tilde{c}_{12}&=1/4(\tilde{c}_{11}+\tilde{c}_{22}+\tilde{c}_{44}+\tilde{c}_{55}+\tilde{c}_{14}+\tilde{c}_{41}\\
&\quad+\tilde{c}_{25}+\tilde{c}_{52}-\tilde{c}_{12}-\tilde{c}_{21}-\tilde{c}_{24}-\tilde{c}_{42}-\tilde{c}_{15}-\tilde{c}_{51}-\tilde{c}_{45}-\tilde{c}_{54}).
\end{aligned} \tag{16}$$

Taking into account Eq. (5), $-4N\beta^{-1}a_1$ is the same as the total energy of a system in which the effective positive charges are placed on 1, 1′, 4, and 4′, negative charges on 2, 2′, 5, and 5′, and nothing on the others. This energy can be calculated using the Ewald method,[11] and the calculated values are

$$\begin{aligned}
a_1&=43160 \text{ K}/T,\\
a_2&=34212 \text{ K}/T,\\
a_3&=38106 \text{ K}/T,\\
a_4&=7428.9 \text{ K}/T.
\end{aligned} \tag{17}$$

With the above, the low-temperature ordered state is the Szabó D state where only one Szabó sublattice (say 1 and 1′) is predominantly occupied and the others have small occupancies with $n_4=n_{4'}$ and $n_{2(2')}=n_{3(3')}=n_{5(5')}=n_{6(6')}$. The D state is found to be stable up to about 6600 K which is far above the melting temperature of AgI (830 K). This disagrees strongly with the result in Ref. 8 where the disordered state is stable above $\sim$400 K, and the ordered state is M below that temperature. The above approach gives such a high transition temperature because the $c_{i1,i1}$ has been assumed to be zero instead of a large negative number, as can be seen from the following calculations.

Let us employ instead the HNC approximation, which is more sophisticated than the above simple mean-field approximation. Our system is the same as a lattice one-component plasma because Ag^+ ions do not feel the structure of the I^- lattice (every Ag^+ site is equivalent). It is known that the HNC closure is a very good approximation in the continuous one-component plasma problem.[12] The one-component plasma parameter here is $\gamma=\beta(Ze)^2/a_{\mathrm{WS}}=23468$ K$/T$ where a_{WS} is the radius of the Wigner-Seitz cell. The lattice Ornstein-Zernike equation for the disordered system[10] is

$$h_{i1,jL}=c_{i1,jL}-\frac{\delta_{ij}\delta_{1L}}{1-n_0}+n_0\sum_k\sum_M\left(c_{i1,kM}-\frac{\delta_{ik}\delta_{1M}}{1-n_0}\right)h_{kM,jL}, \tag{18}$$

and the lattice analog of the HNC closure is

$$c_{i1,jL}=-\beta v_{i1,jL}-\ln(h_{i1,jL}+1)+h_{i1,jL}, \tag{19}$$

where $h_{i1,jL}=g_{i1,jL}-1$. We follow the iterative method of Ref. 13 to solve the above equations. With an initial guess of $h_{i1,jL}$, the $c_{i1,jL}$ are calculated from Eq. (19) and

$$c_{i1,i1}=-\frac{n_0}{1-n_0}\sum_{j\neq i}\sum_{L\neq 1}c_{i1,jL}h_{jL,i1}. \tag{20}$$

The $h_{i1,jL}$ and $c_{i1,jL}$ thus obtained are inserted in the following equation:

$$h_{i1,jL}=\frac{1}{(1-n_0)^{-1}-n_0c_{i1,i1}} \times\left[c_{i1,jL}+n_0\sum_{k\neq i}\sum_{M\neq 1}c_{i1,kM}h_{kM,jL}\right], \tag{21}$$

and the new trial $h_{i1,jL}$ is

$$h_{i1,jL}^{\text{new}}=(t)h_{i1,jL}+(1-t)h_{i1,jL}^{\text{guess}}, \tag{22}$$

where $0<t<1$ is chosen to achieve a faster convergence. The system size needed to assure convergence ranges from $|\mathbf{r}_{\max}|=4a$ for 900 K to $6a$ for 350 K. In solving the equations, $h_{i1,jL}$ is assumed to be zero for $|\mathbf{r}|>|\mathbf{r}_{\max}|$, but long-ranged $c_{i1,jL}=-\beta v_{i1,jL}$ are included for this range. Because the system is not spherically symmetric, the correlation functions depend on direction as well as distance, as can be seen from the multivalued nature of the distribution function in Fig. 4(a). The distinct separations that give different values of the pair-correlation function were determined by considering the symmetry of the lattice and using $g_{iL,jM}=g_{jM,iL}$. The correlation functions have been calculated before[14] for a similar model, but with an approximation that they depend only on distance.

The parameters a_1-a_4 are calculated from an Ewald summation of the $-\beta v_{i1,jL}$ term and a direct summation of the remaining terms in Eq. (19). The calculated values for 500 K, for example, are

$$\begin{aligned} a_1&=3.1606,\\ a_2&=5.3797,\\ a_3&=2.9644,\\ a_4&=-1.1831. \end{aligned} \tag{23}$$

These are far smaller in magnitude than those in Eq. (17). However, the ordered phase obtained is once again the D phase, not M, and no intermediate phase was found. The transition temperature is about 350 K.

IV. MONTE CARLO SIMULATION

As a complementary way to calculate the correlation functions and a direct way to study phase transitions, we performed lattice Monte Carlo simulations on this system. A cubic simulation box with sides of $8a$ which consists of 1024 Ag^+ ions was used. It is larger than the size used in Ref. 8 where the box size was $(6a)^3$. The side should be an even multiple of a in order for the periodic boundary condition to be consistent with the existence of an M phase. The energy of the system is calculated using the Ewald method, considering all periodic images of the ions in a background of opposite charge.[15] In order to save computation time, Ewald energies for all the different separations of pairs of Ag^+ ions are calculated in advance and referred to later in the simulation cycles. The correlation functions can be calculated for $|\mathbf{r}|<4a$. Those at 900 K are shown in Fig. 4(b) and compared with those from the above HNC calculation [Fig. 4(a)] and Ref. 8 [Fig. 4(c)]. The distance at which $g(r)$ has its maximum value calculated from HNC ($r=\sqrt{10}/4a$) is slightly smaller than that from MC and Ref. 8 ($r=\sqrt{12}/4a$).

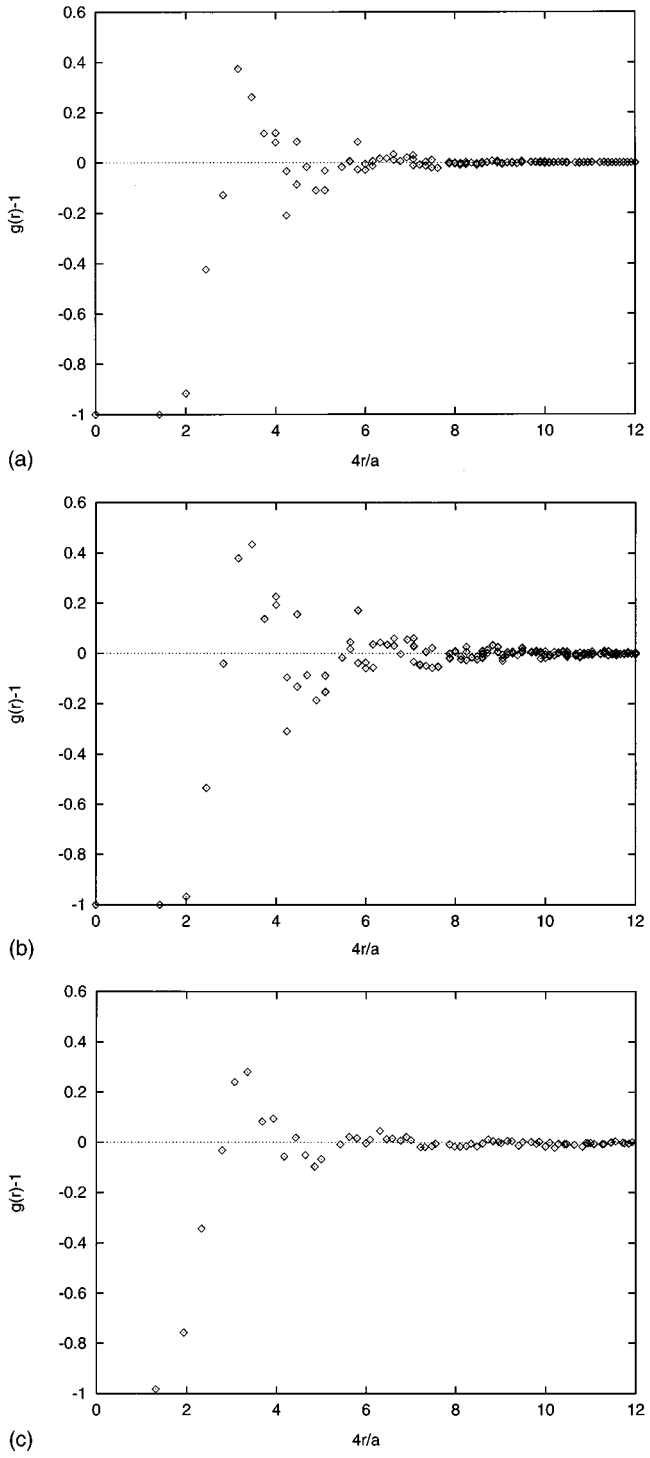

FIG. 4. Pair correlation functions at 900 K calculated from (a) the HNC closure, (b) Monte Carlo simulation, and (c) from Ref. 8.

A similar shift occurs in the continuous system.[16] Note that the D phase has the first peak of $g(r)$ at $r=\sqrt{12}/4a$. Also, the amplitude of $g(r)$ from HNC is smaller than from MC, as in the continuous case.[12]

An ordered phase with the bcc structure was obtained below ~ 700 K, significantly higher than that obtained from the HNC density-functional calculation. One can understand this from the behavior of the pair-correlation functions in Fig. 4. The fact that the low-temperature phase is D, not M, is also expected from the fact that the perfectly ordered D phase, where the Ag^+ ion structure has the same symmetry as the I^- lattice, has lower energy than M ($E_M - E_D = 1.204$ kJ/mol).

One might think that because the tetrahedral sites are occupied by only 70% at ~ 400 K,[8] and even fewer at higher temperatures, interactions with other sites might favor the M phase. We investigated this possibility by including the trigonal interstitial sites that lie half-way between neighboring tetrahedral sites. The occupancy of the tetrahedral sites at high temperature from simulation is similar to that found in Ref. 8, but it increases as the temperature is lowered and the system goes to a phase similar to D at ~ 600 K. This extension of the simulation thus still does not account for the observation of the M phase in Ref. 8. In fact, a trigonal site is not a potential well, but a saddle point in passing from one T_d site to another.[17] It is usually thought that sites other than T_d are on the paths for motion of Ag^+ ions among T_d sites.

V. DEFORMATION OF THE I^- LATTICE

It has been shown that our model gives the D phase at low temperature instead of Madden's M phase, although neither Madden's model nor ours allows bcc–hcp transformation of the I^- lattice. Our lattice approximation for Ag^+ ions does not seem to explain the difference, in view of the calculations just mentioned that include the trigonal sites. Here we discuss the possibility that a change of the structure of the I^- lattice occurred in the simulation of Ref. 8, as well as in real AgI.

In Ref. 8, it was argued that the M phase is unstable with respect to the deformation shown in Fig. 3(a) [gliding of alternate (110) planes of I^-], which would lead to the stable β phase, if the stress imposed by the boundary condition is relaxed; therefore, the ordering of Ag^+ ions drives the transition to the β phase. The M phase is transformed to the β phase by a glide of $\delta=\sqrt{2}/8a$ and a small change in the size and shape of the unit cell. We note that the deformation of Fig. 3(a) can occur without violating the periodic cubic boundary condition in the simulation. If this deformation is favored energetically, it might be responsible for the transition to the M phase in Ref. 8. We calculated the energies of the perfectly ordered M phase when the I^- lattice is deformed and Ag^+ ions are kept tetrahedrally coordinated to I^- ions. The result obtained by Eq. (14) and the Ewald summation for each potential energy term[15] is shown in Fig. 5. The energy for a deformed M phase is lower than that of the D phase for a narrow range around $\delta=0.15a$. Therefore, one can understand that the D phase is stable in our model because such a deformation is not allowed, whereas the M phase obtained in Ref. 8 may have actually a slightly deformed I^- structure. However, it is difficult to tell from Figs. 7 or 8 of Ref. 8 whether there is a small deformation of $\delta\sim 0.15a$ because of large fluctuations in the position of ions. If the ordering of Ag^+ ions in the M phase is accompanied by the structural deformation of the I^- lattice, the $\alpha-\beta$ transition is not driven by the former alone, as suggested by Madden *et al.*, but both changes play a role in the transition.

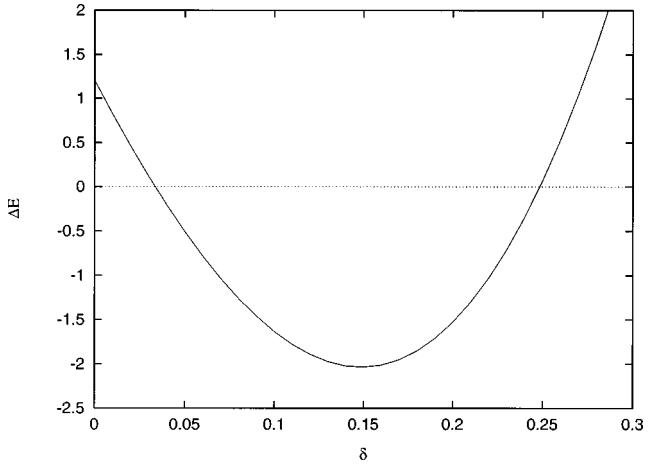

FIG. 5. Energy of the deformed M phase, ΔE, versus degree of deformation δ. Zero of the energy corresponds to the energy of the D phase.

We now proceed further to suggest that the same kind of deformation may be related to the proposed order-disorder transition seen experimentally within the α phase. If a small deformation of the I^- lattice occurs in the α phase, the T_d sites are no longer equivalent, and different sites will have different occupancies. However, the state can be still considerably disordered, giving high conductivity. The transition from the isotropic high temperature α phase to an anisotropic disordered or partially ordered phase with a deformed I^- lattice is consistent with Raman-scattering experiments.[2] The above proposition is also consistent with the fact that the $\alpha-D$ transition temperature ($T_{\alpha-D}$) is very high ($\sim$ 700 K) from the above MC simulation. Because the deformed M phase has lower energy than D, the expected $\alpha-M$ transition temperature is higher than $T_{\alpha-D}$, which is already higher than $T_{\alpha-M}\sim 400$ K from Ref. 8. However, if there exists an intermediate phase between α and M, the transition temperature to M can be lower than $T_{\alpha-D}$.

In the intermediate phase, the I^- lattice of α-AgI will not be the bcc, but a deformed bcc just above the $\alpha-\beta$ transition temperature ($T_{\alpha-\beta}$), although the deformation will be very small ($\delta<0.15a$). The structure of AgI just above $T_{\alpha-\beta}$ was determined by Strock[18] using x-ray scattering. He analyzed the data in terms of the possible peaks for a unit cell that consists of 16 molecules (a bcc unit cell has two), and found that the positions of strong peaks are consistent with the bcc structure. However, the deformation $\delta<0.15a$ is so small that the extra peaks for a deformed bcc will have intensities less than 3% of the highest peak, and those peaks will be very broad because the gliding of (110) planes is a soft mode.[20] Therefore, deformation of the I^- lattice may not have been noticed in the above and later experiments. If such a structural change occurs, there must also be a change in Bragg peak intensities when plotted against temperature, but

no appreciable change was found in x-ray[19] and neutron-scattering[20] experiments. However, the small change predicted in the peak intensity ($<3\%$) would have been extremely hard to detect.

VI. A FORMALISM INCORPORATING THE DEFORMATION

Although change of density and shape of the cell are not allowed, incorporation of the deformation discussed above [gliding of alternate (110) planes of I^- and accompanied change of T_d sites] is important in understanding the mechanism of the $\alpha-\beta$ transition and the intermediate phase in the α phase. We discuss a formalism incorporating the deformation, but the calculation has not yet been carried out.

The free energy is now a function of $\{n_i\}$ and δ:

$$F(\{n_i\},\delta)=F_{\mathrm{AgAg}}(\{n_i\},\delta)+E_{\mathrm{AgI}}(\{n_i\},\delta)+E_{\mathrm{II}}(\delta). \tag{24}$$

E_{II} is the interaction energy between I^- ions, and $E_{\mathrm{AgI}}=N\Sigma_i\epsilon_i n_i$ where ϵ_i is the potential at site i due to the I^- lattice. Although E_{II} and E_{AgI} are infinite, the difference between the free energies of different states can be calculated. The free energy due to the interactions of silver ions F_{AgAg} can be calculated by a method similar to Sec. II. The symmetry of the lattice has changed, and the coordinates of the T_d sites now depend on δ. The 12 sublattices are not equivalent to each other any more, and there are three groups of different sublattices: $\{1,3',4,6'\}$, $\{1',3,4',6\}$, and $\{2,2',5,5'\}$. Because of the reduced symmetry, there are 20 different $\overline{c_{ij}}$'s instead of the 11 in Sec. II ($\overline{c_{11}}$, $\overline{c_{12}}$, $\overline{c_{13}}$, $\overline{c_{14}}$, $\overline{c_{16}}$, $\overline{c_{11'}}$, $\overline{c_{12'}}$, $\overline{c_{13'}}$, $\overline{c_{14'}}$, $\overline{c_{16'}}$, $\overline{c_{1'1'}}$, $\overline{c_{1'2'}}$, $\overline{c_{1'4'}}$, $\overline{c_{1'2}}$, $\overline{c_{1'3}}$, $\overline{c_{1'6}}$, $\overline{c_{22}}$, $\overline{c_{22'}}$, $\overline{c_{25}}$, $\overline{c_{25'}}$), and eight linear combinations of them, b_1-b_8, must be calculated:

$$\begin{aligned}
b_1&=\overline{c_{11}}+\overline{c_{13'}}-\overline{c_{12}}-\overline{c_{12'}},\\
b_2&=\overline{c_{11}}+\overline{c_{13'}}-\overline{c_{11'}}-\overline{c_{13}},\\
b_3&=\overline{c_{11}}+\overline{c_{13'}}-\overline{c_{14}}-\overline{c_{16'}},\\
b_4&=\overline{c_{11}}+\overline{c_{13'}}-\overline{c_{14'}}-\overline{c_{16}},\\
b_5&=2\overline{c_{12}}+2\overline{c_{12'}}-\overline{c_{22}}-\overline{c_{22'}}-\overline{c_{25}}-\overline{c_{25'}},\\
b_6&=\overline{c_{11}}+\overline{c_{13'}}-\overline{c_{1'2}}-\overline{c_{1'2'}},\\
b_7&=\overline{c_{11}}+\overline{c_{13'}}-\overline{c_{1'1'}}-\overline{c_{1'3}},
\end{aligned} \tag{25}$$

$$b_8=\overline{c_{11}}+\overline{c_{13'}}-\overline{c_{1'4'}}-\overline{c_{1'6}},$$

to evaluate

$$\begin{aligned}
\sum_j \overline{c_{1(3')j}}(n_j-n_0)&=2b_1w+b_2x+b_3y+b_4z,\\
\sum_j \overline{c_{2(2',5,5')j}}(n_j-n_0)&=b_5w+(b_6-b_1)(x+z),\\
\sum_j \overline{c_{3(1')j}}(n_j-n_0)&=2(b_6-b_2)w+(b_7-b_2)x+(b_4-b_2)y\\
&\quad+(b_8-b_2)z,\\
\sum_j \overline{c_{4(6')j}}(n_j-n_0)&=2(b_1-b_3)w+(b_4-b_3)x-b_3y\\
&\quad+(b_2-b_3)z,\\
\sum_j \overline{c_{6(4')j}}(n_j-n_0)&=2(b_6-b_4)w+(b_8-b_4)x+(b_2-b_4)y\\
&\quad+(b_7-b_4)z.
\end{aligned} \tag{26}$$

The number of distinct separations $\mathbf{r}$ for which pair-correlation functions should be calculated is now 2951 and 9807 for $|\mathbf{r}_{\max}|=4a$ and $6a$, respectively, compared to 302 and 936 when there is no deformation. If the HNC closure is to be used, ten times more computation time is required for a state with fixed T and δ, and it will take a considerable amount of time to search for free-energy minima in the two-dimensional space of temperature and δ. Moreover, the problem of finding the free energies of the reference states with different lattice structures must be solved, although they may be assumed to be the same in a first-order approximation. In an MC simulation, the homogeneous reference state may not be stable because the sublattices are not equivalent, so a different technique should be used. This calculation will be carried out in the future.

ACKNOWLEDGMENTS

This work was supported by the National Science Foundation through Grant No. CHE 9422999 and through the Materials Research Science and Engineering Center at the University of Chicago. Early conversations about this problem with Paul Madden, and early contributions to the calculation by Robert Mashl, are gratefully acknowledged.

[1] C. M. Perrott and N. H. Fletcher, J. Chem. Phys. **50**, 2770 (1969).
[2] A. Fontana and G. Mariotto, Phys. Rev. B **21**, 1102 (1980); G. Mariotto, A. Fontana, E. Cazzanelli, F. Rocca, M. P. Fontana, V. Mazzacurati, and G. Signorelli, *ibid.* **23**, 4782 (1981).
[3] L. Börjesson and L. M. Torell, Phys. Rev. B **36**, 4915 (1987).
[4] B.-E. Mellander, Phys. Rev. B **26**, 5886 (1982).
[5] M. Parrinello, A. Rahman, and P. Vashishta, Phys. Rev. Lett. **50**, 1073 (1983).
[6] J. L. Tallon, Phys. Rev. B **38**, 9069 (1988).
[7] G. Szabó, J. Phys. C **19**, 3775 (1986).
[8] P. A. Madden, K. O'Sullivan, and G. Chiarotti, Phys. Rev. B **45**, 10 206 (1992).
[9] W. G. Burgers, Physica (Utrecht) **1**, 561 (1934).
[10] M. Nieswand, W. Dieterich, and A. Majhofer, Phys. Rev. E **47**, 718 (1993).
[11] M. P. Allen and D. J. Tildesley, *Computer Simulation of Liquids* (Oxford, New York, 1987).
[12] J. F. Springer, M. A. Pokrant, and F. A. Stevens, Jr., J. Chem. Phys. **58**, 4863 (1973).
[13] E. Scalas and R. Ferrando, Phys. Rev. E **49**, 513 (1994).

[14] R. Zimmermann and R. Zeyher, Solid State Commun. **40**, 441 (1981).
[15] J. P. Hansen, Phys. Rev. A **8**, 3096 (1973).
[16] K.-C. Ng, J. Chem. Phys. **61**, 2680 (1974).
[17] F. Billi, H. E. Roman, and W. Dieterich, Solid State Ion. **28–30**, 58 (1988).
[18] L. W. Strock, Z. Phys. Chem. Abt. B **25**, 441 (1934).
[19] S. Hoshino, J. Phys. Soc. Jpn. **12**, 315 (1957).
[20] V. M. Nield, D. A. Keen, W. Hayes, and R. L. McGreevy, Solid State Ion. **66**, 247 (1993).